Dynamic Modeling of a Poppet Valve for use in a Rotating Spool Compressor

International Compressor Engineering Conference at Purdue, July 11-14, 2014

Nathaniel Wood
Torad Engineering
Cumming, Georgia

Craig R. Bradshaw, PhD
Torad Engineering LLC
Cumming, Georgia

Joe Orosz
Torad Engineering LLC
Cumming, Georgia

Greg Kemp
Torad Engineering LLC
Cumming, Georgia

Eckhard A. Groll, PhD
Ray W. Herrick Laboratories and Cooling Technologies Research Center
West Lafayette, Indiana

Dynamic Modeling of a Poppet Valve for use in a Rotating Spool Compressor

Nathaniel Wood[1], Craig R. Bradshaw[1], Joe Orosz[1*], Greg Kemp[1], Eckhard A. Groll[2]

[1]Torad Engineering
Cumming, GA, USA
Phone – (770-889-8400), Fax – (770-889-6900), E mail – joe.orosz@toradengineering.com

[2]Ray W. Herrick Laboratories, West Lafayette, IN 47907
Phone – (765-496-2201). Fax – (765-494-0787), E mail – groll@purdue.edu

[*]Corresponding Author

ABSTRACT

The operational efficiency of the rotating spool compressor, first introduced by Kemp *et al*. (2008), has been improved in recent years through the modeling of various elements in the compression cycle. In order to continue the advancements of the design, a model for predicting the discharge valve dynamics is introduced. The model is created using high-pressure measurements both upstream and downstream of the valve. The model is able to predict the initial valve displacement with a mean absolute percent error of 6.91%. The model is also able to predict the amount of time the valve is open in one valve oscillation with a mean absolute error of 9.51%.

1. INTRODUCTION

The rotary spool compressor was first introduced by Kemp *et al.* (2008). Since that time, advancements have been made to the rotary spool compressor design. This includes improvements to tip seals, as seen in Kemp *et al*. (2012a), and Bradshaw (2013) and spool seals, as seen in Kemp *et al*. (2012b). Additional changes have come about through the comprehensive modeling of the rotary spool compressor (Bradshaw and Groll, 2013) and the losses through various elements in the compressor (Bradshaw *et al*., 2016). The ability to model any losses in the compressor allows for a focused approach on which elements in the rotary spool compressor design need improvements.

The work in Bradshaw *et al.* (2016) identified the discharge process as a significant loss in the compression cycle of the rotary spool compressor. This includes any losses due to flow through the discharge port, any losses derived from the valve motion, and any losses caused by backflow through the discharge valve. The ability to understand how a valve will behave without testing it in the compressor would be useful as a design tool. This would allow for a fast and effective way to improve the discharge process and reduce the associated losses.

Reducing discharge losses in the compressor is assisted by modeling the initial opening displacement of the discharge valve. By modeling the initial displacement of a certain discharge valve system, the valve performance can be established for a certain set of discharge conditions. This is done by seeing how quickly the valve reaches the stop and how the valve reacts after hitting the stop. If the valve rapidly hits the stop and returns with a high velocity towards the seat, it would be expected that the valve would continue in this state of motion until the entire discharge process ended. On the other hand, if the model shows the valve hitting the stop and then coming to rest on the stop, this would indicate that the valve setup was performing in a nearly ideal manner.

Using a self-acting poppet valve in an HVAC&R compressor is uncommon. The poppet valve is used in the spool compressor to lower clearance volume and to decrease leakage around the tip seal. The most commonly used self-acting valve used is the reed valve. The functional difference between a reed valve and a poppet valve is the way in which the spring force is applied. A poppet valve consists of two main parts: the valve body and the external spring; whereas, the reed valve consists only of a valve body that includes the spring force by way of the deflection of the

valve body material. This allows for less components for a reed valve configuration and ultimately a lower mass, leading to its wide use in the compressor industry. This becomes more evident when looking for previous documentation on modeling valve dynamics. Previous investigations into the discharge valve dynamics were conducted where pressures around the valve were found using an analytical approach. This approach can be seen in Benson and Ucert (1972), where the pressures acting on the valve are found using a combination of the energy and continuity equations. By using high-speed pressure measurements, a more accurate relationship between the pressures acting on the valve and its accompanying dynamics could be found. In order to fully understand the valve dynamics in a rotary spool compressor, this work developed an experimental environment to study the valve movement under various pressure loads.

2. EXPERIMENTAL SETUP

2.1 Discharge Valve Apparatus

The test apparatus was designed to simulate the discharge process of a rotary spool compressor in a more controlled fashion than the compressor itself can yield. The test apparatus simulates the two discharges of gas per shaft revolution, intrinsic to the spool compressor. The working fluid of the testing apparatus was compressed air instead of refrigerant. An assembly and section view of the final test apparatus is shown in Figure 1. The testing apparatus consists of four main parts: the rotor housing, the rotor, the valve seat plate, and the discharge plenum. The rotor housing includes an inlet port with an accompanying channel to supply compressed air to the valve. The inlet and discharge ports are located on opposite sides of the housing and offset from each other. The top of the rotor housing has a port to allow gas entering into the housing to travel into the valve seat plate. The rotor is manufactured of PEEK and includes two through holes placed perpendicular to each other and offset 29 mm in order for each hole to access either the inlet channel or the discharge channel in the housing. In the valve seat plate, there is a cavity upstream of the valve to allow for a larger volume of air. There is also a pressure tap located in the valve seat plate to allow for the upstream pressure measurement of the valve. The discharge plenum consists of the valve guide and stop, as well as a discharge port to allow flow through the valve and a pressure tap for measuring the downstream pressure.

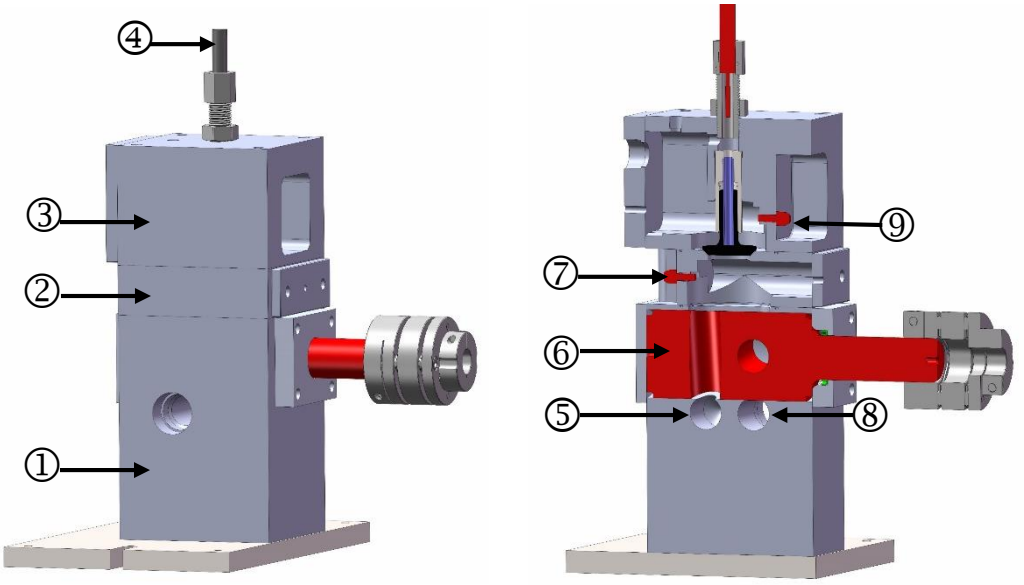

Figure 1: (left) Assembly view of the testing apparatus. (right) Section view of the testing apparatus. (1) rotor housing (2) valve seat plate (3) discharge plenum (4) LVDT (5) compressed air inlet (6) rotor (7) upstream pressure sensor (8) atmosphere vent (9) downstream pressure sensor

2.2 Experimental Measurements

The upstream and downstream pressures were measured using high-speed pressure sensors located in both the valve seat plate and the discharge plenum as shown in Figure 1, as described above. The two high-speed pressure sensors used in the testing apparatus were the Endevco Model 8530b-500 sensors. The upstream and downstream pressures were sampled at 50 kHz to capture any rapid changes in the pressures.

To capture the valve motion, a linear variable differential transformer (LVDT) was used. The armature was attached to the valve by the addition of a threaded hole to the valve face, where the armature for the LVDT could be threaded into the valve. To ensure the security of the armature to the valve, a jam nut was added to the threaded armature as shown in Figure 2. The LVDT used in this experiment was the Daytronic DS400SUHA. The LVDT was also sampled at a rate of 50 kHz.

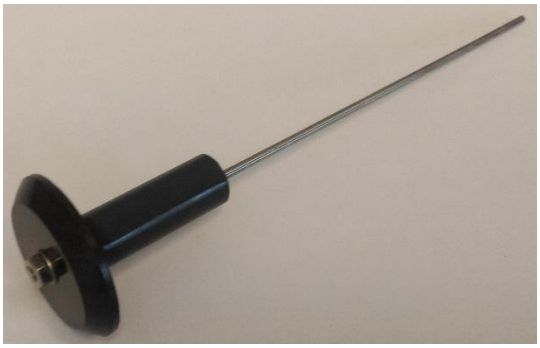

Figure 2: Valve body with attached LVDT armature

Along with the pressure measurements and displacement measurement described above, inlet pressure and temperature were collected. The pressure transducer and thermocouple were located in the inlet manifold adjacent to the apparatus. The pressure transducer used for the inlet was the Omega PX4202-600G5V and the thermocouple used was the Omega TMQSS-125U-6. The inlet temperature and pressure were sampled at 50 Hz.

2.2.1 Experimental Uncertainty

The absolute uncertainty for the Endevco Model 8530b-500 high-speed pressure sensor is ± 17 kPa. The absolute uncertainty associated with the LVDT, the DS400SUHA, is ± 0.05 mm. The absolute uncertainty for the PX4202-600G5V pressure transducer and the TMQSS-125U-6 thermocouple is ± 10 kPa and ± 0.50 °C, respectively.

2.3 Experimental Procedure

In order to fully capture the operating conditions that could be encountered during the discharge cycle of a spool compressor, inlet pressures and shaft speeds were varied. Five different inlet pressures were tested, ranging from 260 kPa to 430 kPa. In addition, five different shaft speeds were used ranging from 600 RPM to 1800 RPM in increments of 300 RPM. These testing points were repeated using five different spring rates. The full test matrix is shown in Table 1 below.

Table 1: Full test matrix; repeated for spring rates of 950, 1400, 1900, 2800, and 3300 N/m

	Shaft Speed (RPM)				
	600	**900**	**1200**	**1500**	**1800**
Inlet Pressure (kPa)	260	260	260	260	260
	300	300	300	300	300
	340	340	340	340	340
	390	390	390	390	390
	430	430	430	430	430

3. VALVE MODEL

3.1 Mechanical Model

The discharge valve system behaves as a single degree of freedom system due to the valve guide only allowing motion in a single direction. Damping forces were not directly accounted for even with the understanding that oil and friction between the valve post and valve guide were present. This allows for a simplification of the model and only a single empirically tuned coefficient. This is similar to the approach used when modeling reed valves in compressors as seen in Boswirth (1980) and Aigner *et al*. (2005). Bredesen (1974) came to the conclusion that any damping forces present in the valve system are negligible when compared to the gas and spring forces. Based on the aforementioned and the free-body diagram shown in Figure 3, the equation of motion for the valve is as shown in Equation (1).

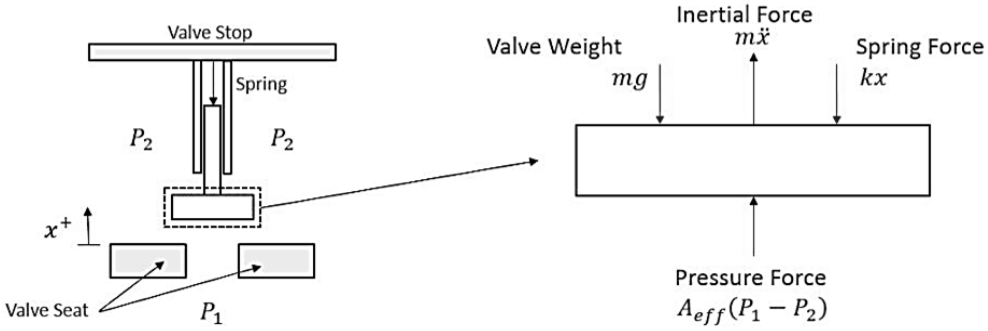

Figure 3: Valve Free Body Diagram

$$m\ddot{x} + k(x + x_0) = A_{eff}\Delta P - mg \tag{1}$$

The total mass, m, is a combination of the mass of the armature and valve as well as the effective spring mass, shown below in Equation (2). The effective spring mass is one-third of the total mass of the spring (Rao, 2004).

$$m = m_v + m_{arm} + \frac{1}{3}m_s \tag{2}$$

The ΔP term in Equation (1) is provided as an input which is found using the dynamic pressure measurements obtained from the test apparatus described in Section 2. The A_{eff} term in Equation (1) represents the effective force area. The effective area is commonly found in many reed valve models. Boswirth (1980) and Benson and Ucert (1972) represents the effective area as a drag coefficient multiplied by the valve disc area. The effective force area accounts for energy loss due to changes in the fluid flow as the valve opens.

3.2 Model Solver

The equation of motion was solved numerically using the fourth-order Runge-Kutta method. The collected pressure difference values were interpolated to use as continuous inputs into the equation of motion. The ODE describing the valve motion was solved in MATLAB (2015b) using the 'ode45' solver.

4. RESULTS

4.1 Mechanical Model Validation

To verify the valve model, a step response experiment was conducted on the valve system. The experiment consisted of supplying the valve with an initial displacement and then quickly releasing the valve to allow it to return to its equilibrium position. This test was conducted without any flow present to ensure correct functioning of the solver and to guarantee an accurate mechanical description of the valve motion. Without flow, there is confidence that any discrepancies in the model predictions is most likely related to the flow and/or pressure fields surrounding the valve, given the accurate prediction of valve displacement considering only the mechanical phenomena. The modeled

displacement exhibited the same rise time and settling time as well as the same overshoot and number of oscillations as the experimentally collected displacement, shown in Figure 4.

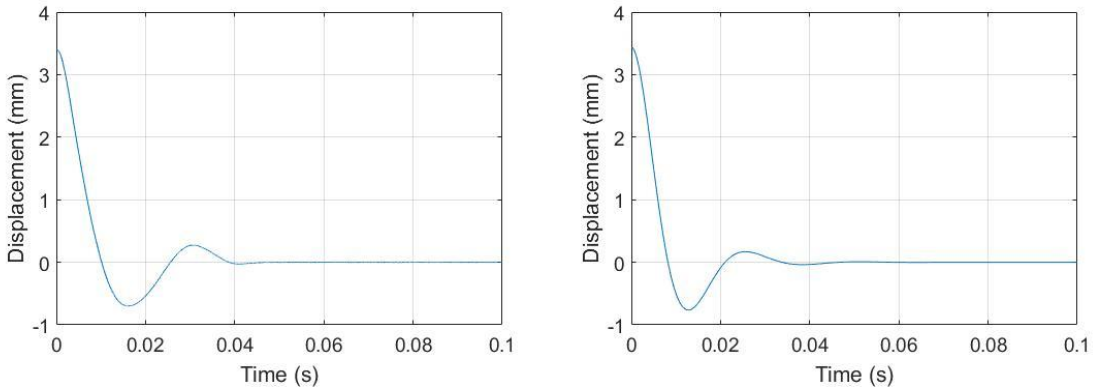

Figure 4: Mechanical step response of the actual system (left) and the model (right)

4.2 Effective Area Estimation

The effective force area for each collected point was found by tuning the model output to produce an initial valve displacement that matched the experimental valve displacement. Figure 5 shows the tuned effective area for each point plotted against the maximum pressure difference reached before the valve opened. This figure shows a wide variation in the effective area for each spring rate.

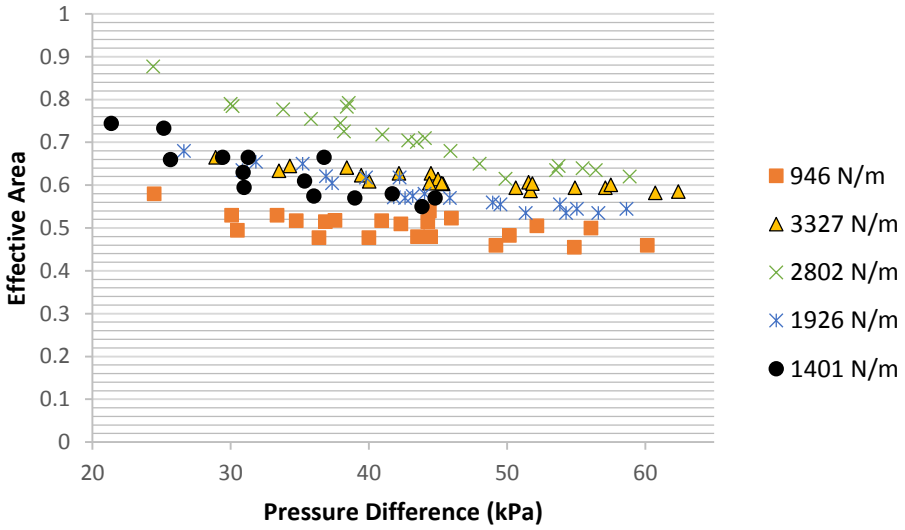

Figure 5: Effective area plotted against opening pressure difference

The values presented in Figure 5 were averaged based on the springs used. With the averaged effective areas, a linear equation was fit to the data and used to predict average effective areas based on the spring rate as shown in Figure 6. This trend allows for a reasonable approximation of the average effective area that would be expected for a given spring rate.

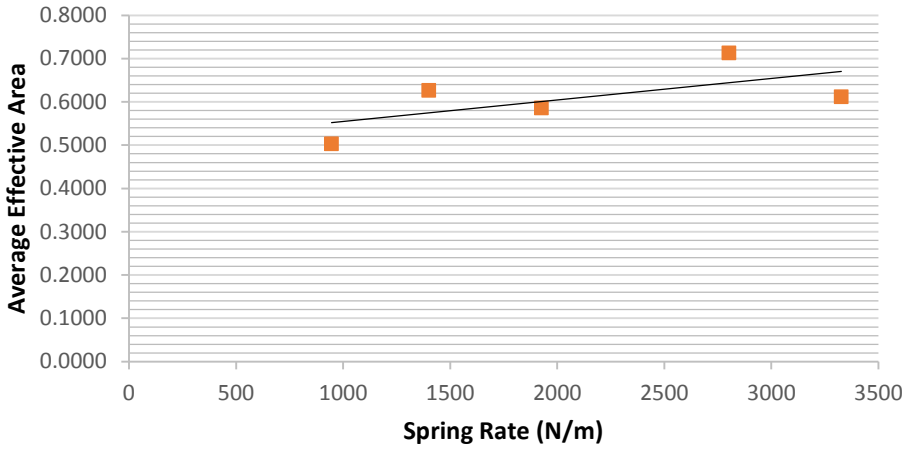

Figure 6: Average effective area plotted against spring stiffness

4.3 Model Validation

The mean absolute percent error of the model's predicted initial valve displacement came out to 6.91%. This value was calculated by taking the percent error between the predicted and the experimentally obtained displacements at each test point. These errors were then averaged to give the final error percentage.

Figure 7 shows the amount of time, for a single oscillation, the valve was open predicted by the model compared to the experimentally collected data. The parity plot includes all testing points introduced in Table 1 of Section 2. The opening time was defined as the difference in time between when the valve initially lifts off the seat and when the valve fully comes to rest on the seat. The model predicts the opening time within a 9.51% mean absolute error.

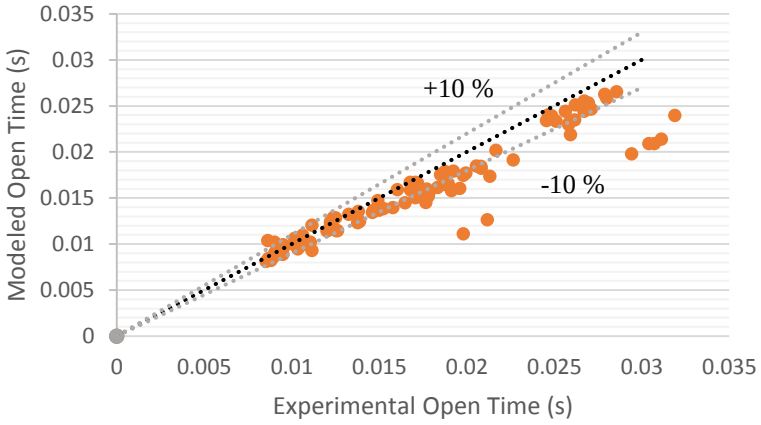

Figure 7: Parity plot of predicted and experimental open times for a single valve oscillation. The upper bound represents a +10% error and the lower bound represents a -10% error.

4.4 Model Strengths

The plots shown in Figure 8 represent points where the model can accurately predict the discharge valve displacement. Figure 8(a) shows the model predicted valve displacement with an inlet pressure of 300 kPa, a shaft speed of 1500 RPM, and a spring rate of 950 Newtons per meter. Figure 8(b) shows the model predicted valve displacement for an inlet pressure of 260 kPa, a shaft speed of 1200 RPM, and a spring rate of 1900 Newtons per meter. Figure 8(c) shows the model predicted valve displacement for an inlet pressure of 300 kPa, a shaft speed of 1200 RPM, and a spring rate of 1400 Newtons per meter. Figure 8(d) shows the model predicted valve displacement for an inlet pressure of 390

kPa, a shaft speed of 1800 RPM, and a spring rate of 2800 Newtons per meter. The model best predicts the valve motion at higher shaft speeds. As the shaft speed increases, the amount of time the valve is exposed to the pressure force decreases. This leads to a lower number of valve oscillations, where the flow does not have enough influence from the oscillating valve body to become as irregular. The valve simply opens due to the initial pressure force and then hits the stop, and then returns to the seat.

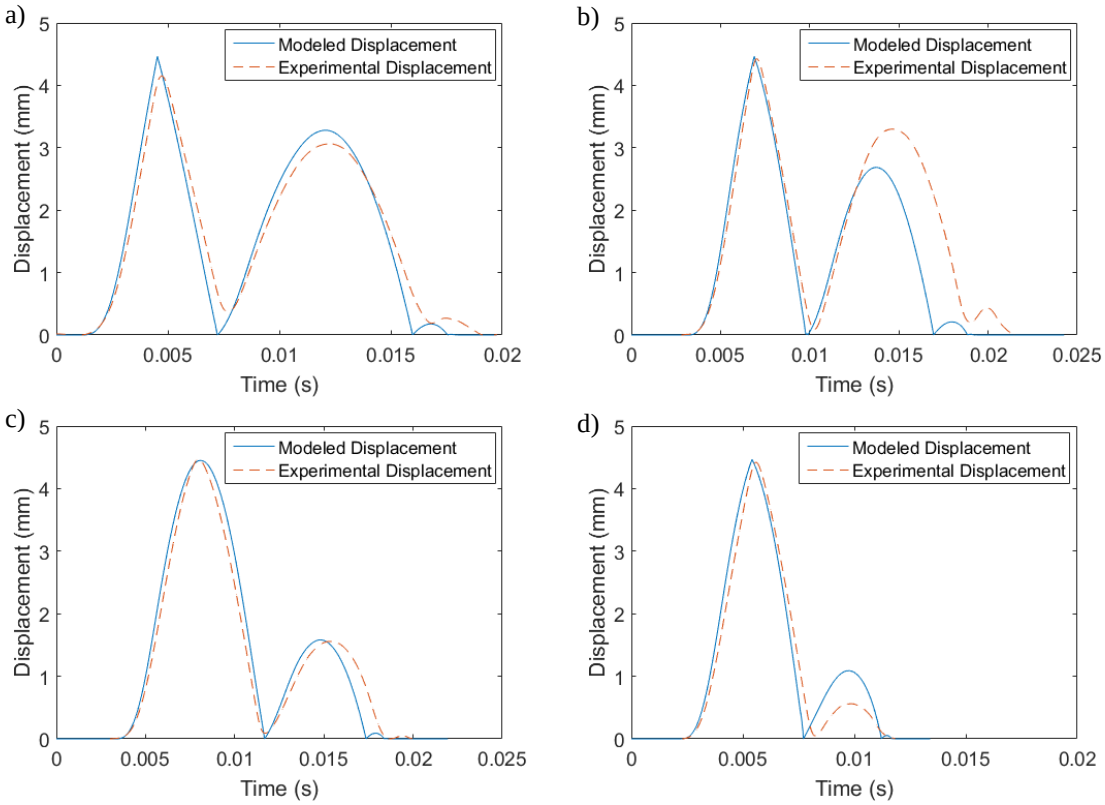

Figure 8: Model predicted valve displacement plotted against experimental valve displacement

4.5 Model Weaknesses

The plots shown in Figure 9 represent points where the model is not able to accurately predict the discharge valve displacement. Figure 9(a) shows the model predicted valve displacement with an inlet pressure of 260 kPa, a shaft speed of 600 RPM, and a spring rate of 2800 Newtons per meter. Figure 9(b) shows the model predicted valve displacement for an inlet pressure of 260 kPa, a shaft speed of 600 RPM, and a spring rate of 950 Newtons per meter. Figure 9(c) shows the model predicted valve displacement for an inlet pressure of 260 kPa, a shaft speed of 600 RPM, and a spring rate of 1400 Newtons per meter. Figure 9(d) shows the model predicted valve displacement for an inlet pressure of 300 kPa, a shaft speed of 600 RPM, and a spring rate of 1900 Newtons per meter.

These plots show the poor prediction capabilities of the model particularly when the shaft speed is below 900 RPM. At lower speeds, the valve is exposed to the pressure force for a relatively long duration. This forces the valve to oscillate, which is caused by the valve trying to reach its equilibrium position based on the pressure and flow acting on it. This oscillation, sometimes called fluttering, additionally causes rapid changes in the pressures surrounding the valve. This oscillation in the flow field becomes very irregular when compared to the flow experienced by the valve when it first opens. These irregular flow fields lead to difficulty in obtaining the measured pressures which can lead to an inaccurate prediction of the dynamics. This suggests, in order to fully describe the valve dynamics at such a shaft speed, more details about the flow around the valve would need to be explained.

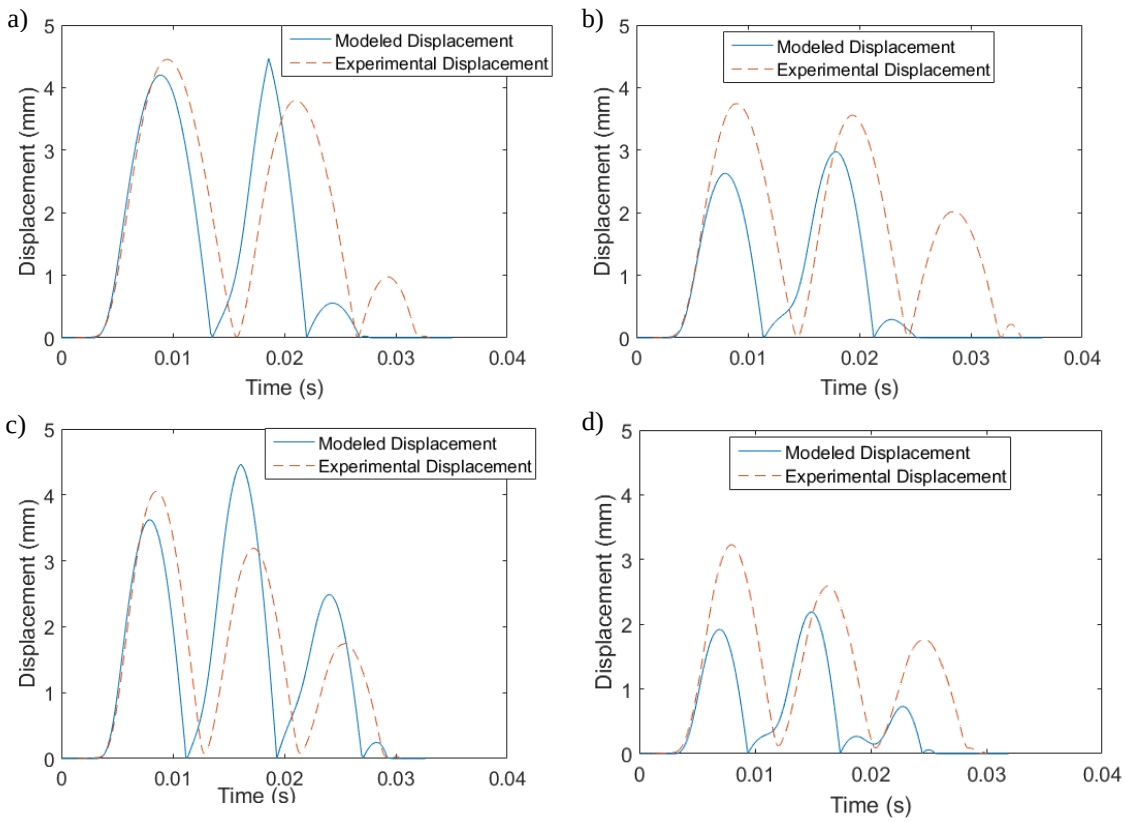

Figure 9: Model predicted valve displacement plotted against experimental valve displacement

5. CONCLUSIONS

5.1 Summary

A model predicting the discharge valve displacement has been presented. The model used high speed pressure measurements upstream and downstream of the valve and also the experimentally discovered relationship of the average effective area and spring rate to predict the discharge valve displacement. The model preforms reasonably well at higher shaft speeds. At lower speeds, the valve displacement is not accurately predicted due to flow forces that were not accounted for.

5.2 Future Work

In order for this model to be useful for future design considerations, the model must be verified by the experimentation of more valve masses. Flow characteristics must be accounted for to accurately predict valve displacements at lower shaft speeds. The addition of more spring rates would increase the confidence in the average effective area trend. Finally, this model will be integrated into the comprehensive model previously presented by Bradshaw and Groll (2013).

NOMENCLATURE

m	mass	(kg)
$\ddot{x}$	valve acceleration	(m/s^2)
x	valve displacement	(m)
k	spring rate	(N/m)

g	acceleration due to gravity	(m/s^2)
A_{eff}	effective area	(m^2)
ΔP	pressure difference	(kPa)

Subscript

v	valve
arm	armature
s	spring

REFERENCES

Aigner, R., Meyer, G., & Steinrück, H. (2005). Valve dynamics and internal waves in a reciprocating compressor. In *4th Conference of the European Forum for Reciprocating Compressors*. pages 169-178.

Benson, R. S., & Ucert, A. S. (1972). A theoretical and experimental investigation of a gas dynamic model for a single stage reciprocating compressor with intake and delivery pipe systems. *Journal Mechanical Engineering Science*, 14(4), 264–279.

Boswirth, L. (1980). Flow forces and the tilting of spring loaded valve plates - part I. In *International Compressor Engineering Conference at Purdue University*. number 330.

Bradshaw, C. R. (2013). Spool Compressor Tip Seal Design Considerations. In *2013 International Conference on Compressors and Their Systems.*

Bradshaw, C. R., & Groll, E. A. (2013). A comprehensive model of a novel rotating spool compressor. *International Journal of Refrigeration*, 36(7), 1974–1981.

Bradshaw, C. R., Kemp, G., Orosz, J., & Groll, E. A. (2016). Development of a loss pareto for a rotating spool compressor using high-speed pressure measurements and friction analysis. *Applied Thermal Engineering*, 99, 392–401.

Bradshaw, C. R., Kemp, G., Orosz, J., and Groll, E. A. (2014). Loss analysis of rotating spool compressor based on high-speed pressure measurements. In *International Compressor Engineering Conference at Purdue University*. number 2271.

Bredesen, A. M. (1974). Computer simulation of valve dynamics as an aid to design. In *International Compressor Engineering Conference at Purdue University*. number 117.

Kemp, G., Orosz, J., Bradshaw, C., and Groll, E. A. (2012a). Spool compressor tip seal design considerations and testing. In *International Compressor Engineering Conference at Purdue University*. number 2079.

Kemp, G., Orosz, J., Bradshaw, C., and Groll, E., A. (2012b). Spool seal design and testing for the spool compressor. In *International Compressor Engineering Conference at Purdue University*, number 2080.

Kemp, G.T., Garrett, N., Groll, E. A., (2008). Novel rotary spool compressor design and preliminary prototype performance, In *International Compressor Engineering Conference at Purdue University*, number 1328.

MATLAB, MATLAB version 8.6.0 (2015b), The MathWorks, Inc., Natick, Massachusetts, United States.

Rao, S. S., 2004. Mechanical Vibrations, 4th Edition. Prentice Hall.